A Study of Ferroelectric Properties of the Oscillator Model of PZT-22

Ikechi Augustine Ukaegbu and Vladimir Nikolaevich Borodulin

In this letter, we study the contemporary technologies for making ferroelectric films and the possibility of using the oscillator model of PZT-22 to analyze its ferroelectric properties. The material showed permittivity dispersion at 65 KHz and 88.5 KHz. We obtained relative attenuation γ, relaxation time τ, and ε_{max} of the material as 0.0008319, 0.5 s, and 603.438, respectively.

Keywords: PZT-22, permittivity dispersion, piezoelectric ceramic.

I. Introduction

The typical properties of ferroelectric films are applied in the construction of nonvolatile memory devices (for example, FeRAM), dynamic random access memory, capacitors, infrared receivers, optical processors, waveguide and delay-circuits (delay-lines), appliances of surface-acoustic waves, and various acoustic devices. The physical properties of the films depend on the state (condition) of the surface, stoichiometry, crystalline nature, thickness, microcrystalline nature, crystallographic orientation, and high processing (that is, methods of obtaining films) temperature [1]. The investigation of dielectric properties in millimeter and sub-millimeter spectral range often provides essential information about the dynamic properties of dielectrics [2].

In this letter, we conduct a brief study of the contemporary technologies of ferroelectric films and the experimental analysis of a PZT-22 ferroelectric disc obtained by a chemical method to check for piezoelectric characteristics.

Manuscript received Apr. 29, 2010; revised Aug. 18, 2010; accepted Sept. 14, 2010.

Ikechi Augustine Ukaegbu (phone: +82 42 350 6269, email: aus20@kaist.ac.kr) is with the Department of Information and Communications Engineering, Korea Advanced Institute of Science & Technology, Daejeon, Rep. of Korea.

Vladimir Nikolaevich Borodulin (email: vnborodulin@mpei.ru) is with the Material Science Engineering Department, Moscow Power Engineering Institute/Technical University, Moscow, Russia.

doi:10.4218/etrij.11.0210.0147

II. Contemporary Technologies of Ferroelectric Films for Non-Volatile Memories and Their Parameters

Nanotechnology in modern nanoelectronics and the possibility of obtaining ultra-thin ferroelectric films are briefly studied. The methods include molecular-beam epitaxy, gas-cycle epitaxy of metal organic compounds, and chemical deposition of surface nanostructures. Contemporary technologies of ferroelectric films for non-volatile memories include magnetron sputtering, laser ablation, and chemical methods [3].

In magnetron sputtering, the target atoms are knocked out by high-energy ions and deposited on the surface of the substrate [4]. Laser ablation focuses the laser beam on the target evaporating atoms and is transferred onto the substrate, where the film is grown. Typically, laser ablation uses powerful lasers with pulse repetition rate from 10 Hz to 100 Hz, operating on the boundaries between electronic levels of excimers, existing only in the electronic excited states. In comparison with the magnetron sputtering method, these methods offer the potential to reduce the temperature of the substrate (which is critical for the integration of ferroelectric films with semiconductors) and to ensure satisfactory completion of stoichiometry conditions of the entire deposition surface. The main difficulty is associated with deposition of homogeneous films on large area substrates and to protect the surface of the growing film from damage by fragments of a decaying target. In chemical vapor deposition of organometallic compounds, streams of gases containing all the necessary components of ferroelectric compounds are focused on the surface of the heated substrate

and react, resulting in the formation of solid ferroelectric films [4]. There are many advantages to using the chemical method [4], [5]: reduction of the substrate temperature (<600°C), ensuring high-quality coatings on large area, high growth rate, preserving the stoichiometry, achieving a high degree of purity and homogeneity of doping, possibility of obtaining films of different thicknesses (from tenths and hundredths of a micron to hundreds of microns) on odd-shaped substrates, reduction of temperature and time of synthesis of the oxide phase, high processability index, and simplicity of equipment.

III. Permittivity Dispersion

The dependence of permittivity with frequency of an alternating field can be described as permittivity dispersion and is represented as in [6]:

$$\varepsilon(\omega)=\varepsilon'(\omega)+i\varepsilon''(\omega)=\varepsilon(\infty)+\frac{\left[\varepsilon(0)-\varepsilon(\infty)\right]\left[1-\left(\frac{\omega}{\omega_0}\right)^2\right]}{\left[1-\left(\frac{\omega}{\omega_0}\right)^2\right]^2+\gamma^2\left(\frac{\omega}{\omega_0}\right)^2}, \quad (1)$$

$$\omega_0=\sqrt{c/m}, \quad (2)$$

$$\gamma=\lambda/\omega_0, \quad (3)$$

where ε' represents permittivity, ε'' is the coefficient of dielectric loss, ω_0 is the natural frequency of the oscillator, c is the elastic constant, m is the mass of an oscillating charge q, γ is the relative attenuation, and λ is frictional force constant arising from various mechanisms of dissipation. The nature (behavior) of the permittivity dispersion is determined by the process of establishing the polarization with time [7]. If the process of polarization is relaxational as in Fig. 1(a), then the dispersion will have the form shown in Fig. 2. When the period of oscillation of the electric field is large compared to the relaxation time τ (ω frequency is small compared with $1/\tau$), polarization has time to follow the field, and the behavior of a dielectric in an alternating electric field will not be substantially different from its behavior in a constant field (that is, $\varepsilon'=\varepsilon$ and $\varepsilon''=0$ as in Fig. 1(a)). At frequencies $\omega>>1/\tau$, the dielectric will not be polarized. This means that the amplitude of P is very small compared with the magnitude of the polarization P_0 in a constant field. This further explains that $\varepsilon'\approx1$ and $\varepsilon''\approx0$, and that ε' with increasing frequency varies from ε to 1. In Fig. 2, ε_1 and ε_2 represent the permittivity and coefficient of dielectric loss, respectively. The most dramatic change to ε_1 occurs precisely at the frequencies ω through $1/\tau$. At the same frequencies, ε_2

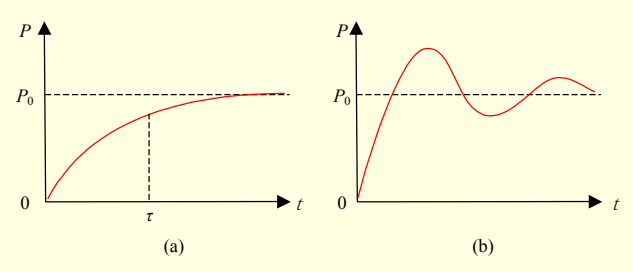

Fig. 1. Two characteristic dependencies of dielectric polarization P with time t. Constant electric field E is applied at time $t=0$ [6].

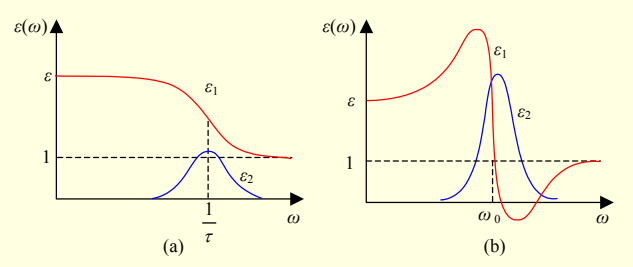

Fig. 2. (a) Relaxation nature of permittivity dispersion of $\varepsilon(\omega)$, which corresponds with dependence $P(t)$, shown in Fig. 1(a), and (b) resonant nature of permittivity dispersion $\varepsilon(\omega)$, which corresponds with dependence on Fig. 1(b) [7].

passes through a maximum point. This pattern of dispersion $\varepsilon(\omega)$ is called relaxation. If the polarization establishment process experiences fluctuations, as shown in Fig. 1(b), then the dispersion of $\varepsilon(\omega)$ will have the form shown in Fig. 2(b). In this case, the nature of the dispersion can be described as a resonance type of dispersion [4].

The value of $\varepsilon''(\omega)$ is always greater than zero, while ε can be positive or negative. When $\omega<\omega_0$, ε' and ε'' increase with frequency within the region $\omega\approx\omega_0$, where they have maximum value. Afterwards, the frequency dependence of ε' and ε'' become different. After reaching the maximum value, ε sharply drops, and at frequency $\omega=\omega_2$, it reaches the minimum value as shown in Fig. 3(a). Then, $\varepsilon'(\omega)$ increases again as it also does when $\omega\to\infty$ and $\varepsilon'\to\infty$. Equations (4) through (8) show the parameters of the oscillator dielectric absorption and dispersion and the relationships between $\varepsilon''(\omega)$, $\tan\delta$, and γ.

$$\varepsilon''(\omega)=\frac{\left[\varepsilon(0)-\varepsilon(\infty)\right]\gamma\frac{\omega}{\omega_0}}{\left[1-\left(\frac{\omega}{\omega_0}\right)^2\right]^2+\gamma^2\left(\frac{\omega}{\omega_0}\right)^2}, \quad (4)$$

$$\tan\delta(\omega)=\gamma\frac{\omega}{\omega_0}\frac{\varepsilon(0)-\varepsilon(\infty)}{\varepsilon(0)}\quad(\omega<<\omega_0), \quad (5)$$

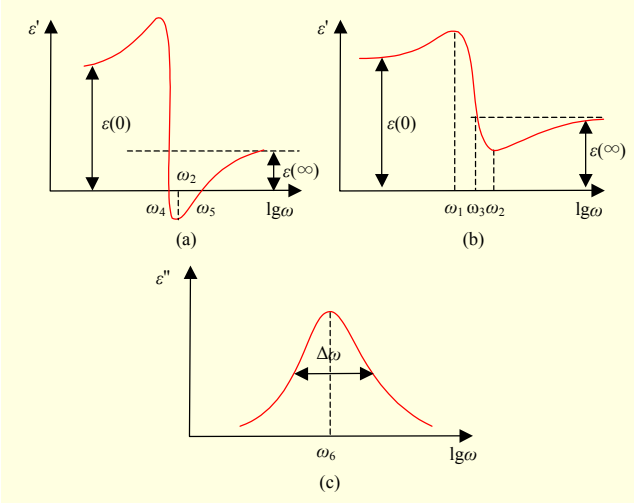

Fig. 3. (a) and (b) Frequency dependence of ε' for different damping and (c) loss factor ε'' of dielectric showing resonance polarization at different parameters of equivalent oscillator [8].

$$\alpha = \frac{\Delta\omega}{2}, \tag{6}$$

$$\tau = \frac{1}{2\alpha}, \tag{7}$$

$$\varepsilon''_{\max}(\omega) = \frac{\varepsilon(0) - \varepsilon(\infty)}{\gamma} \quad (\gamma < 1). \tag{8}$$

IV. Experimental Results

We studied the possibilities of using the oscillator model of the ceramic PZT-22. We also analyzed the results obtained from the PZT-22. A dielectric sample in the form of a monocrystal, ceramic, or film with electrodes, which possesses piezoelectric properties and has a particular geometric form, can be characterized as a piezoelectric resonator. Under testing, the PZT-22 has a circular nature with diameter of 20 mm and thickness of 2 mm. The ceramic PZT-22 is placed between two electrodes: a flat rectangular electrode at the base and a pin-like electrode placed at the center above as shown in Fig. 4. The arrangement of the electrodes is done in such a way as to allow free vibration of the PZT material.

In the piezoelectric resonator, mechanical vibrations can be initiated by applying an electric field to it, and also, mechanical vibrations on the plates of the resonator can excite the electric field (the resonator must have a mechanical connection with the source of vibrations). The main factors determining the behavior of the resonator and its characteristics are the physical parameters of a piezoelectric material, the topology of the electrodes, the dielectric (ferroelectric material), and the

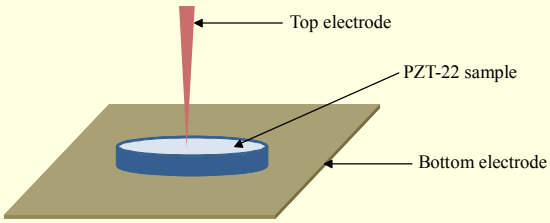

Fig. 4. Diagram illustrating electrode setup for measurement.

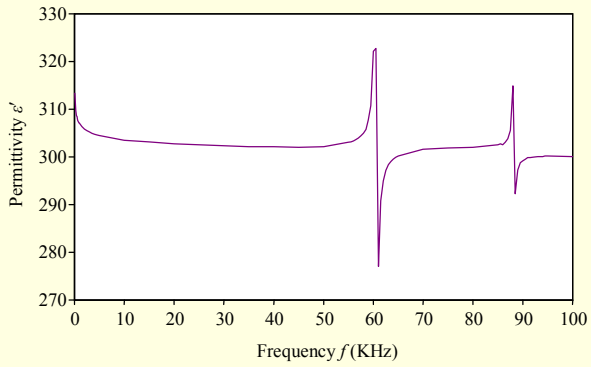

Fig. 5. Dependence of permittivity (ε') with frequency (f) for piezoelectric ceramic (PZT-22).

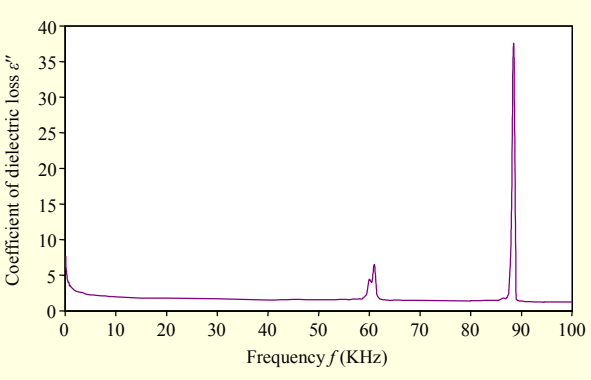

Fig. 6. Dependence of coefficient of dielectric loss (ε'')

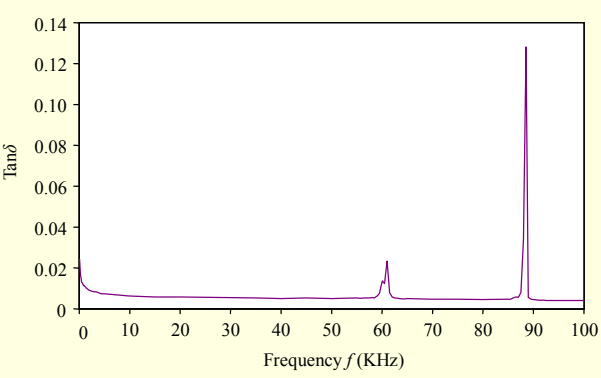

Fig. 7. Dependence of dielectric loss tangent (tanδ) with frequency (f) for piezoelectric ceramic (PZT-22).

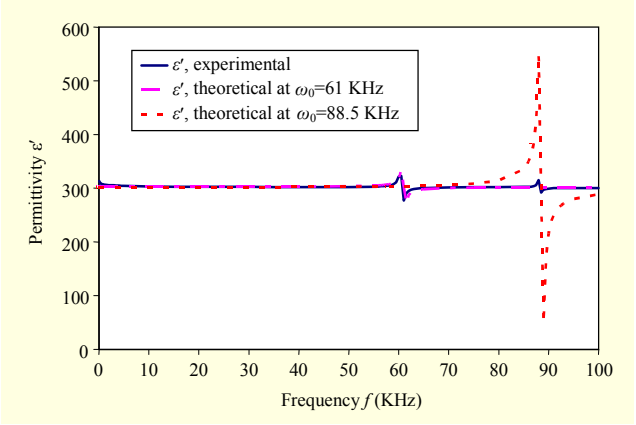

Fig. 8. Experimental and theoretical plots showing dependence of permittivity (ε') with frequency (f) for piezoelectric ceramic (PZT-22).

magnitude and direction of polarization. Permittivity in ferroelectrics is observed at relatively low frequencies (below 10^6 Hz to 10^7 Hz), where it is related to the vibrations of the domain walls. In this work, an electrical field is applied across the electrodes while varying the frequency. We measured the dependence of the capacitance with frequency.

The dependence of dielectric permittivity, tangent of the angle of dielectric loss, and the coefficient of dielectric loss are characterized by the piezoelectric (PZT-22) behavior in an electric field in the frequency range of 0.1 KHz up to 100 KHz. Figure 5 shows the dependence of dielectric permeability (ε') with piezoceramic (PZT-22) frequency (f), and Fig. 6 shows the dependence of the coefficient of dielectric loss (ε'') with frequency (f) of the piezoceramic (PZT-22). Figure 7 shows the dependence of the tangent of dielectric loss ($\tan\delta$) with frequency (f) for the piezoceramic PZT-22.

In Fig. 5, the several areas of permittivity dispersion can be seen at different frequency ranges. The presence of these generally well-defined areas indicates that the polarization of the dielectric is caused by different mechanisms [9].

For our sample, the permittivity dispersion occurred at frequencies of 61 KHz and 88.5 KHz. These frequencies are low and typical of ferroelectrics. The frequency values were used as ω_0 to calculate permittivity theoretically. Figure 8 shows the comparison of experimental results and theoretically (numerically) calculated dependence of ε' with frequency.

From Fig. 8, we can see that the experimental plot is in agreement with the theoretical plot. From (3), (7), and (8), γ, τ, and ε_{max} were found to have values of 0.0008319, 0.5 s, and 603.438, respectively.

V. Conclusion

We briefly studied some contemporary methods for obtaining ferroelectric films. We also studied and analyzed the parameters of the piezoceramic PZT-22 obtained by a chemical method. The results obtained show full agreement with the behavior of ferroelectric materials. The results also indicate the possible use of the material for the fabrication of non-volatile memories.

References

[1] B.M. Goltsman and V.K. Yarmarkin, "Ferroelectric Materials for Dynamic-Memory Integrated Circuits," *Tech. Phys*., vol. 44, no. 5, 1999, pp. 558-561.

[2] G. Kozlov and A. Volkov, *In Millimeter and Sub-millimeter Wave Spectroscopy of Solids*, G. Gruner, Ed. Berlin: Springer, 1998, pp. 51-107.

[3] I.A. Ukaegbu and V.N. Borodulin, "Modern Technologies of Ferroelectric Films for Nonvolatile Memory of Integrated Circuits," *Proc. ISTC*, vol. 2, 2006, p. 58.

[4] A.C. Sigov, "Ferroelectric Thin Films in Microelectronics," *Soroski Edu. J*., no. 10, 1998, pp. 83-91.

[5] V.N. Borodulin, *Active Dielectrics. Ferroelectric Films*, Moscow: Moscow Power Engineering Institute/Technical Press, 2003.

[6] A.M. Loktionov et al., "Dielectric Dispersion in Polymer Ferroelectric Films of Legmyura-Blodgett," *Phys. Solid State*, vol. 48, no. 6, 2006, pp. 1101-1003.

[7] V.N. Borodulin, *Physics of Dielectrics*, Moscow: Moscow Power Engineering Institute/Technical University Press, 1981.

[8] I.S. Rez and Y.M. Poplavko, "M: Radio and Telecommunications," *Dielectrics: Basic Properties and Applications in Electronics*, (Russian), 1989.

[9] I.A. Ukaegbu, *Perspective Technologies of Ferroelectric Films for Non-volatile Memories of Integrated Circuits*, Moscow: Moscow Power Engineering Institute/Technical University Press, 2006.